Electro-Fenton and Photoelectro-Fenton Degradation of Sulfanilic Acid Using a Boron-Doped Diamond Anode and an Air Diffusion Cathode

ARTICLE *in* THE JOURNAL OF PHYSICAL CHEMISTRY A · MARCH 2012

Impact Factor: 2.69 · DOI: 10.1021/jp300442y · Source: PubMed

7 AUTHORS, INCLUDING:

Abdellatif El-Ghenymy
University of Barcelona
17 PUBLICATIONS **191** CITATIONS
SEE PROFILE

Jose Antonio Garrido Ponce
University of Barcelona
126 PUBLICATIONS **3,529** CITATIONS
SEE PROFILE

Pere Lluís Cabot
University of Barcelona
151 PUBLICATIONS **3,970** CITATIONS
SEE PROFILE

THE JOURNAL OF PHYSICAL CHEMISTRY A

Article

pubs.acs.org/JPCA

Electro-Fenton and Photoelectro-Fenton Degradation of Sulfanilic Acid Using a Boron-Doped Diamond Anode and an Air Diffusion Cathode

Abdellatif El-Ghenymy, José Antonio Garrido, Francesc Centellas, Conchita Arias, Pere Lluís Cabot, Rosa María Rodríguez, and Enric Brillas*

Laboratori d'Electroquímica dels Materials i del Medi Ambient, Departament de Química Física, Universitat de Barcelona, Martí i Franquès 1-11, 08028 Barcelona, Spain

ABSTRACT: The mineralization of sulfanilic acid has been studied by electro-Fenton (EF) and photoelectro-Fenton (PEF) reaction with UVA light using an undivided electrochemical cell with a boron-doped diamond (BDD) anode and an air diffusion cathode able to generate H_2O_2. Organics were then oxidized by hydroxyl radicals formed at the anode surface from water oxidation and in the bulk from Fenton's reaction between generated H_2O_2 and added Fe^{2+}. The UVA irradiation in PEF enhanced the production of hydroxyl radicals in the bulk, accelerating the removal of organics and photodecomposed intermediates like Fe(III)−carboxylate complexes. Partial decontamination of 1.39 mM sulfanilic acid solutions was achieved by EF until 100 mA cm^{-2} at optimum conditions of 0.4 mM Fe^{2+} and pH 3.0. The increase in current density and substrate content led to an almost total mineralization. In contrast, the PEF process was more powerful, yielding almost complete mineralization in less electrolysis time under comparable conditions. The kinetics for sulfanilic acid decay always followed a pseudo-first-order reaction. Hydroquinone and *p*-benzoquinone were detected as aromatic intermediates, whereas acetic, maleic, formic, oxalic, and oxamic acids were identified as generated carboxylic acids. NH_4^+ ion was preferentially released in both treatments, along with NO_3^- ion in smaller proportion.

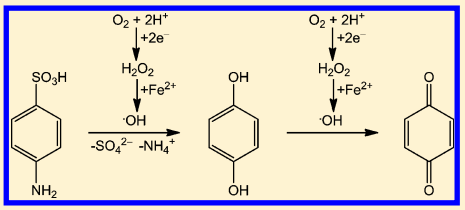

1. INTRODUCTION

A large variety of advanced oxidation processes (AOPs) have been recently applied to the degradation of toxic and/or biorefractory organics in wastewaters.[1−4] These powerful oxidation methods are chemical, photochemical, photocatalytic, and electrochemical processes based on the in situ generation of hydroxyl radical ($^{\bullet}OH$), which is a strong oxidant because of its high oxidation power [$E°(^{\bullet}OH/H_2O)$ = 2.80 V/SHE]. $^{\bullet}OH$ nonselectively reacts with most organics in waters giving rise to dehydrogenated or hydroxylated derivatives, which can be in turn totally mineralized, i.e., transformed into CO_2, water, and inorganic ions. Among these techniques, electrochemical AOPs (EAOPs) have received great attention due to their environmental compatibility, versatility, high efficiency, amenability of automation, and safety because they operate under mild conditions.[5−8]

The most popular EAOP based on Fenton's reaction chemistry is the electro-Fenton (EF) process.[7] In this method, hydrogen peroxide is continuously supplied to a contaminated acidic solution by the two-electron reduction of injected O_2 at the cathode from reaction 1, whereas Fe^{2+} ion is added as catalyst to react with generated H_2O_2 originating homogeneous $^{\bullet}OH$ and Fe^{3+} ion from Fenton's reaction 2:

$$O_2 + 2H^+ + 2e^- \rightarrow H_2O_2 \quad (1)$$

$$Fe^{2+} + H_2O_2 \rightarrow Fe^{3+} + {}^{\bullet}OH + OH^- \quad (2)$$

An advantage of EF compared with the classical chemical Fenton process is that reaction 2 is mainly propagated by the cathodic reduction of Fe^{3+} to Fe^{2+} from reaction 3:[9]

$$Fe^{3+} + e^- \rightarrow Fe^{2+} \quad (3)$$

Good efficient cathodes for H_2O_2 generation from reaction 1 in EF are carbon nanotubes−polytetrafluoroethylene (PTFE),[10,11] carbon nanotubes on graphite,[12] carbon felt,[9,13−17] activated carbon fiber,[18] boron-doped diamond (BDD),[19] and carbon−PTFE gas (O_2 or air) diffusion[20−25] electrodes.

When an undivided cell with a BDD anode is used in EF, organics can be attacked by $^{\bullet}OH$ produced in the bulk from Fenton's reaction 2 and by heterogeneous hydroxyl radical, designed as BDD($^{\bullet}OH$), formed from water oxidation at the anode by reaction 4:[7,21,23]

$$BDD + H_2O \rightarrow BDD({}^{\bullet}OH) + H^+ + e^- \quad (4)$$

BDD thin-film electrodes are the most potent anodes known because they possess an inert surface with low adsorption, remarkable corrosion stability, and extremely wide potential windows (>3 V) in aqueous medium.[5,6,8,26] These properties confer a very weak BDD−$^{\bullet}OH$ interaction that results in a

Received: January 13, 2012
Revised: March 8, 2012
Published: March 12, 2012

higher O_2-overpotential than other anodes like Pt and PbO_2, and in the formation of higher amounts of heterogeneous hydroxyl radicals from reaction 4, which react more rapidly with several aromatics and carboxylic acids.[27−34]

Another interesting EAOP is the photoelectro-Fenton (PEF) process, where the solution is treated under EF conditions and simultaneously irradiated with either artificial UVA light of λ_{max} = 360 nm[7,23−25,35] or sunlight.[35,36] The synergistic oxidative action of this radiation is accounted for by (i) the photolysis of $Fe(OH)^{2+}$, the predominant species of Fe^{3+} in the pH range 2.5−4.0, from reaction 5 producing additional $^{\bullet}OH$ and more Fe^{2+} to catalyze Fenton's reaction 2 and (ii) the photolysis of Fe(III)−carboxylate complexes, as reaction 6 depicts for Fe(III)−oxalate complexes [$Fe(C_2O_4)^+$, $Fe(C_2O_4)_2^-$, and $Fe(C_2O_4)_3^{3-}$]:[37]

$$Fe(OH)^{2+} + h\nu \rightarrow Fe^{2+} + {}^{\bullet}OH \quad (5)$$

$$2Fe(C_2O_4)_n^{(3-2n)} + h\nu \rightarrow 2Fe^{2+} + (2n-1)C_2O_4^{2-} + 2CO_2 \quad (6)$$

Sulfanilic acid (4-aminobenzenesulfonic acid) is widely used to synthesize pesticides, sulfonamide pharmaceuticals, sulfonated azo dyes, dye mordants, species, and food pigments. This toxic and carcinogenic sulfonated amine is accumulated in industrial dye wastewaters, rivers, and surface waters where it is formed, for example, from the reduction of sulfonated azo dyes under anaerobic conditions.[38−40] Sulfanilic acid can be very slowly biodegraded by different bacterial strains under aerobic conditions[41−44] and slowly destroyed by ozonation[45] and anodic oxidation.[46] It has been reported that this compound is generated as intermediate in the degradation of the antimicrobial sulfamethoxazole by TiO_2 photocatalysis[47] and Fenton reagent[48] and in the removal of the dye Acid Orange 7 by anodic oxidation[49] and EF.[14] However, the degradation of sulfanilic acid by EF and PEF has not been described yet in the literature. This research shows the ability of these EAOPs to destroy this compound and its byproduct in environmental waters.

In this paper, we report on an exhaustive study of the EF and PEF treatment of acidic solutions of sulfanilic acid using an undivided BDD/air diffusion cell. The effects of pH, Fe^{2+} concentration, current density, and substrate content on the degradation rate, mineralization degree, and mineralization current efficiency (MCE) were examined for both EAOPs. The decay kinetics of sulfanilic acid and the evolution of its aromatic intermediates, generated carboxylic acids, and released inorganic nitrogen ions were clarified by different liquid-chromatography (LC) techniques.

2. EXPERIMENTAL SECTION

2.1. Chemicals. Reagent grade sulfanilic acid (>99% purity) was purchased from Sigma-Aldrich and used without further purification. Hydroquinone and *p*-benzoquinone were of reagent grade supplied by Panreac and Merck, respectively. Maleic, acetic, formic, oxalic, and oxamic acids were of reagent grade purchased from Avocado and Panreac. Sulfuric acid, anhydrous sodium sulfate, and ferrous sulfate heptahydrate were of analytical grade supplied by Merck and Fluka. Solutions were prepared with high-purity water obtained from a Millipore Milli-Q system with resistivity >18 MΩ cm at 25 °C. Organic solvents and other chemicals used were of either HPLC or analytical grade purchased from Aldrich, Fluka, and Avocado.

2.2. Electrolytic Systems. All electrolyses were conducted in an open and undivided cylindrical tank reactor of 150 mL capacity surrounded with a double jacket for circulation of external thermostated water to regulate the solution at 35 °C using a Thermo Electron Corp. HAAKE DC 10 thermostat. The anode was a BDD electrode purchased from Adamant Technologies (La-Chaux-de-Fonds, Switzerland), which was synthesized by the hot filament chemical vapor deposition technique on single-crystal *p*-type Si(100) wafers (0.1 Ω cm, Siltronix). The cathode was a carbon−PTFE air-diffusion electrode supplied by E-TEK (Somerset, NJ) and mounted as described elsewhere.[50] The geometric area of all electrodes in contact with the solution was 3 cm^2. The air diffusion cathode was fed with 300 mL min^{-1} of air with a pump to produce H_2O_2 from reaction 1. All the assays were performed at constant current density provided with an Amel 2053 potentiostat−galvanostat. Before the electrolytic trials, the BDD anode and the air diffusion cathode were polarized in a 0.05 M Na_2SO_4 solution at 100 mA cm^{-2} for 60 min for their activation and removal of the surface impurities.

Comparative EF and PEF treatments were made using 100 mL of sulfanilic acid solutions in 0.05 M Na_2SO_4 as background electrolyte. The effects of pH between 2.0 and 6.0, Fe^{2+} concentration up to 1.0 mM, applied current density between 33.3 and 150 mA cm^{-2}, and sulfanilic acid content from 1.39 to 13.9 mM on the degradation rate, mineralization degree, and decay kinetics of the substrate were examined for both EAOPs. In all cases, the treated solution was stirred with a magnetic bar at 700 rpm to ensure its mixing and the transport of reactants toward/from the electrodes. For the PEF process, the solution was irradiated with a Philips TL/6W/08 fluorescent black light blue tube of 320−400 nm with λ_{max} = 360 nm, placed at the top of the open cell at 7 cm above the solution, giving a photoionization energy input of 5 W m^{-2}, as detected with a Kipp & Zonen CUV5 radiometer.

2.3. Instruments and Product Analysis Procedures. The solution pH was measured with a Crison GLP 22 pH-meter. Aliquots withdrawn from electrolyzed solutions were alkalinized to quench the Fenton process and filtered with 0.45 μm PTFE filters from Whatman before analysis. The mineralization of sulfanilic acid solutions was monitored from their total organic carbon (TOC) decay, determined with a Shimadzu VCSN TOC analyzer. Reproducible TOC values with an accuracy of ±1% were found by injecting 50 μL aliquots to the analyzer. The MCE value for each trial at current I (A) and time t (h) was then estimated by eq 7:[51]

$$MCE = \frac{nFV_s\Delta(TOC)_{exp}}{4.32 \times 10^7 mIt} \times 100 \quad (7)$$

where F is the Faraday constant (96 487 C mol^{-1}), V_s is the solution volume (L), $\Delta(TOC)_{exp}$ is the experimental solution TOC decay (mg L^{-1}), 4.32×10^7 is a conversion factor to homogenize units (3600 s h^{-1} × 12000 mg mol^{-1}), and m is the number of carbon atoms of sulfanilic acid (6). The number of electrons (n) consumed per each substrate molecule was taken as 28, assuming that it is completely mineralized to carbon dioxide and sulfate and ammonium ions from reaction 8:

$$C_6H_7NO_3S + 13H_2O \rightarrow 6CO_2 + NH_4^+ + SO_4^{2-} + 29H^+ + 28e^- \quad (8)$$

dx.doi.org/10.1021/jp300442y | J. Phys. Chem. A 2012, 116, 3404−3412

The formation of sulfate ion is expected from the oxidation behavior of sulfonated compounds,[14,22] whereas the initial nitrogen is mainly converted into NH_4^+ ion, as will be discussed below.

The evolution of aromatic intermediates was followed by reversed-phase HPLC using a Waters 600 LC fitted with a Thermo Electron Corp. Hypersil ODS [5 μm, 150 mm × 3 mm (i.d.)] column at room temperature and coupled with a Waters 996 photodiode array detector set at the maximum wavelength of the UV spectrum of each compound, that is, λ = 289 nm for hydroquinone and λ = 246 nm for *p*-benzoquinone. The mobile phase was a 5:95 (v/v) acetonitrile/water (phosphate buffer, pH 3) mixture at 0.6 mL min^{-1}. The decay kinetics for sulfanilic acid and the time course of generated carboxylic acids were followed by ion-exclusion HPLC using the above LC fitted with a Bio-Rad Aminex HPX 87H [300 mm × 7.8 mm (i.d.)] column at 35 °C and the photodiode array detector selected at λ = 249 nm for sulfanilic acid and λ = 210 nm for aliphatic carboxylic acids, using 4 mM H_2SO_4 at 0.6 mL min^{-1} as mobile phase. The NH_4^+ concentration in electrolyzed solutions was found by ionic chromatography with a Shimadzu 10 Avp LC fitted with a Shodex IC YK-421 [125 mm × 4.6 mm (i.d.)] cation column at 40 °C coupled with a Shimadzu CDD 10 Avp conductivity detector. The mobile phase was a 5.0 mM tartaric acid, 2.0 mM dipicolinic acid, 24.2 mM boric acid, and 15.0 mM crown ether solution at 1.0 mL min^{-1}. The NO_3^- content was obtained by the same technique using a Shim-Pack IC-A1S [100 mm × 4.6 mm (i.d.)] anion column at 40 °C and a mobile phase composed of 2.4 mM tris(hydroxymethyl)aminomethane and 2.5 mM phthalic acid circulating at 1.5 mL min^{-1}.

3. RESULTS AND DISCUSSION

3.1. Effect of pH and Fe^{2+} Concentration on TOC Removal by EF. The solution pH affects the rate of Fenton's reaction 2, so it is usually found that in the EF process organics are more quickly removed by •OH in the pH interval 2.0−4.0.[7] To confirm this behavior for the EF treatment of sulfanilic acid, a series of experiments was carried out by electrolyzing solutions containing 1.39 mM of this compound (equivalent to 100 mg L^{-1} TOC) and 0.4 mM Fe^{2+} at pH ranging between 2.0 and 6.0 in the BDD/air diffusion cell by applying 66.6 mA cm^{-2} for 360 min. While the pH of solutions with initial pH ≤3.0 remained practically unchanged during electrolysis, the solutions with pH ≥4.0 were strongly acidified, probably due to the formation of short-linear carboxylic acids,[7,23−25] and then their pH was continuously adjusted to their initial value by adding small volumes of 0.1 M NaOH. Figure 1a shows a progressive TOC removal with prolonging electrolysis time for all pH values tested, although a partial mineralization was always obtained. Thus, at the end of such experiments, the TOC was reduced by 83%, 85%, 77%, 74%, and 68% for increasing pH values of 2.0, 3.0, 4.0, 5.0, and 6.0. These results evidence that a greater mineralization degree was achieved in the pH range 2.0−3.0, although the pH 3.0 was optimal for the EF degradation of sulfanilic acid, a value close to the optimum pH of 2.8 for Fenton's reaction 2.[2,3] This finding suggests that •OH formed from this reaction is the main oxidizing agent of sulfanilic acid and its intermediates in the EF process, because the generation of the oxidant BDD(•OH) from reaction 4 is expected to be pH independent.[8] Nevertheless, the fact that only partial mineralization is achieved by EF is indicative of the formation of very refractory byproducts that are difficultly oxidized by both •OH and BDD(•OH).

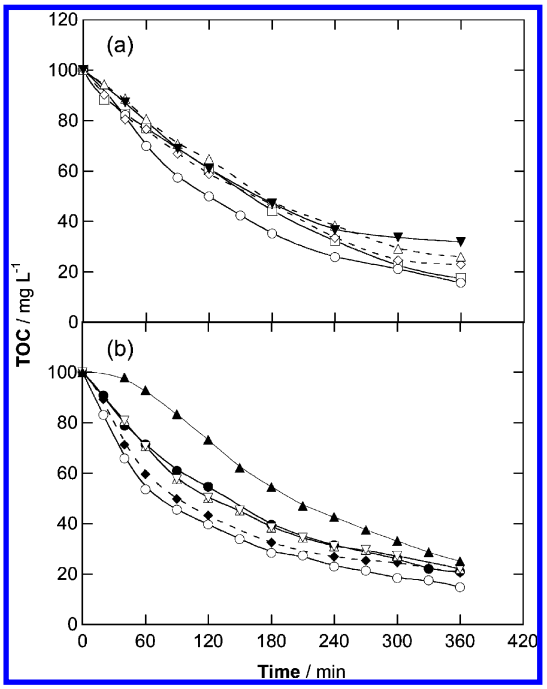

Figure 1. Effect of (a) pH and (b) Fe^{2+} concentration on TOC removal with electrolysis time for the electro-Fenton (EF) degradation of 100 mL of 1.39 mM sulfanilic acid solutions in 0.05 M Na_2SO_4 using an open and undivided cylindrical cell with a 3 cm^2 boron-doped diamond (BDD) anode and a 3 cm^2 air diffusion cathode at 66.6 mA cm^{-2} and 35 °C. In plot a, pH = (□) 2.0, (○) 3.0, (◇) 4.0, (Δ) 5.0, and (▼) 6.0 and $[Fe^{2+}]_0$ = 0.4 mM. In plot b, pH = 3.0 and $[Fe^{2+}]_0$ = (▲) 0 mM, (●) 0.2 mM, (○) 0.4 mM, (◆) 0.6 mM, (Δ) 0.8 mM, and (▽) 1.0 mM.

The predominant oxidation role of •OH in EF was corroborated by studying the influence of Fe^{2+} catalyst. This was made by determining the comparative TOC decay of a 1.39 mM sulfanilic acid solution containing Fe^{2+} concentrations up to 1.0 mM at the optimum pH 3.0 and 66.6 mA cm^{-2}. As can be seen in Figure 1b, the use of anodic oxidation (without Fe^{2+}), where only BDD(•OH) is formed from reaction 4, allowed 75% mineralization after 360 min of electrolysis. The S-shaped TOC−*t* plot found under these conditions indicates the existence of a lower reactivity of organics with BDD(•OH) at the beginning of the process, which is enhanced at longer electrolysis by the formation of species that are more easily destroyed by this oxidant. In contrast, Figure 1b evidences that the presence of Fe^{2+} in the medium always causes a much quicker TOC removal at the initial stages and a greater final mineralization degree owing to the much faster removal of organics by the action of •OH in EF. The gradual addition of Fe^{2+} up to 0.4 mM raises the degradation rate as a result of the acceleration of Fenton's reaction 2 producing greater amounts of •OH. However, an increase from 0.4 to 1.0 mM Fe^{2+} causes a progressive inhibition of the process, which can be related to the loss of •OH by reaction with the excess of added Fe^{2+} from the waste reaction 9:[7]

$$Fe^{2+} + {}^{\bullet}OH \rightarrow Fe^{3+} + OH^- \quad (9)$$

The above considerations indicate that pH 3.0 and 0.4 mM Fe^{2+} are optimal for the EF process of sulfanilic acid and then both conditions were taken to study the comparative TOC abatement by EF and PEF at different current densities and substrate concentrations, as discussed in the subsection below.

3.2. Influence of Current Density and Sulfanilic Acid Content on the Comparative TOC Removal by EF and PEF.

The current density is a key parameter in EAOPs because it regulates the production of generated oxidants [•OH and BDD(•OH)]. Parts a and b of Figure 2 illustrate the TOC decay for a 1.39 mM sulfanilic acid solution at optimum 0.4 mM Fe^{2+} and pH 3.0 by EF and PEF, respectively, at constant current density from 33.3 to 150 mA cm^{-2} for 360 min as maximal. In all cases, the pH was not regulated because it slightly decreased to 2.7−2.9 at the end of treatment. As can be seen, the TOC was removed more rapidly with raising current density in both EAOPs, although a greater mineralization degree was always attained for PEF. At 300 min, for example, TOC was reduced by 72%, 79%, 80%, and 92% in EF and 92%, 95%, 96%, and 97% in PEF for increasing current densities of 33.3, 66.6, 100, and 150 mA cm^{-2}. The higher oxidation power of PEF leading to an almost total mineralization can be accounted for by the potent action of UVA light, which can be due to the generation of greater amounts of •OH from Fenton's reaction 2 induced by the photolytic reaction 5 and/or the photodecomposition of complexes of Fe(III) with intermediates like short-linear carboxylic acids.[7,23−25]

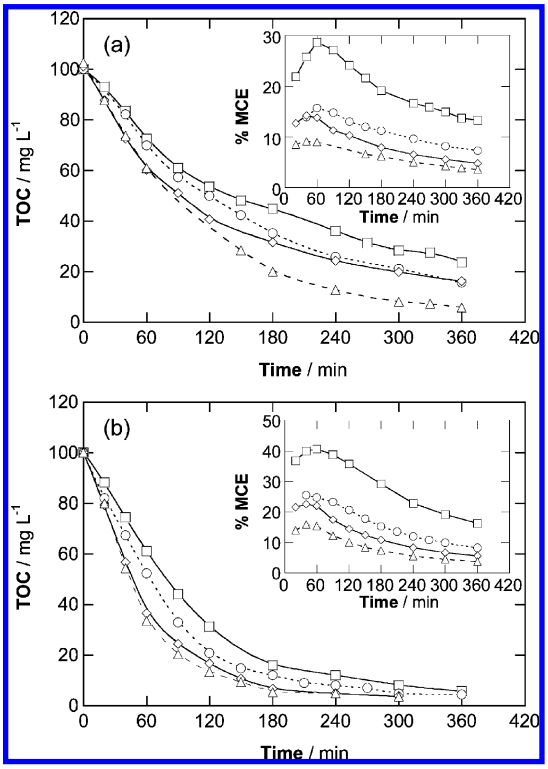

Figure 2. Influence of current density on TOC abatement with electrolysis time for (a) EF and (b) photoelectro-Fenton (PEF) treatments of 100 mL of a 1.39 mM sulfanilic acid solution in 0.05 M Na_2SO_4 with 0.4 mM Fe^{2+} at pH 3.0 and 35 °C. Applied current density: (□) 33.3 mA cm^{-2}, (○) 66.6 mA cm^{-2}, (◇) 100 mA cm^{-2}, and (△) 150 mA cm^{-2}. Each inset panel illustrates the corresponding mineralization current efficiency calculated from eq 7. The PEF processes were carried out under 6 W UVA irradiation of λ_{max} = 360 nm.

The effect of current density on the degradation rate of both EF and PEF processes can be better analyzed from their MCE values calculated from eq 7. The inset panel of Figure 2a evidences the existence of a maximum efficiency at about 60 min for EF, which decayed from 28% at 33.3 mA cm^{-2} to 9% at 150 mA cm^{-2}. The same behavior can be observed in the inset panel of Figure 2b for PEF, although with greater maximum efficiencies varying between 41% at 33.3 mA cm^{-2} and 15% at 150 mA cm^{-2}. The loss in efficiency at long electrolysis time can be mainly associated with the concomitant decrease in organic matter in solution.[8] Note that increasing current density causes a greater production of •OH, since more H_2O_2 is generated at the air diffusion cathode by reaction 1 enhancing Fenton's reaction 2,[7,51] as well as of BDD(•OH), since water oxidation at the BDD anode by reaction 4 is accelerated.[8,33] The higher production of both oxidants with increasing current density then explains the quicker TOC decay shown in Figure 2a,b for both EAOPs. However, the dramatic fall in their MCE values indicates that the increase in current is mainly consumed in parasitic nonoxidizing reactions of hydroxyl radicals, because organic pollutants react very hardly with them. Some examples of such waste reactions are the direct oxidation of BDD(•OH) to O_2 via reaction 10, the dimerization of •OH to H_2O_2 by reaction 11, and its destruction either with Fe^{2+} by reaction 9 or H_2O_2 by reaction 12 giving rise to the weaker oxidant hydroperoxyl radical ($HO_2^•$):[7,8,26,34]

$$2BDD(^•OH) \rightarrow 2BDD + O_2(g) + 2H^+ + 2e^- \quad (10)$$

$$2\,^•OH \rightarrow H_2O_2 \quad (11)$$

$$H_2O_2 + \,^•OH \rightarrow HO_2^• + H_2O \quad (12)$$

Moreover, BDD(•OH) generation can also be inhibited by the parallel production of weaker oxidants like $S_2O_8^{2-}$ ion from SO_4^{2-} ion oxidation by reaction 13 and O_3 by reaction 14:[6,8]

$$2SO_4^{2-} \rightarrow S_2O_8^{2-} + 2e^- \quad (13)$$

$$3H_2O \rightarrow O_3(g) + 6H^+ + 6e^- \quad (14)$$

The influence of sulfanilic acid concentration on the oxidation power of both EAOPs was also examined. To do this, solutions up to 13.9 mM of this compound with 0.4 mM Fe^{2+} were comparatively degraded at pH 3.0 and 66.6 mA cm^{-2}. Figure 3a evidences the great oxidation ability of EF for concentrated solutions. After 360 min of this treatment, about 85% of TOC was removed for all contents. By prolonging the electrolysis, an almost total mineralization with 95% TOC abatement was achieved at 480 min for 6.95 mM and at a longer time of 540 min for 13.9 mM due to the presence of more recalcitrant organic matter. This behavior is reflected in the large increase found in MCE from 15% for 1.39 mM to 60% for 13.9 mM, as can be seen in the inset panel of Figure 3a. Since the same current density was applied in these trials, similar amounts of •OH and BDD(•OH) are expected to be produced for all substrate contents. The greater efficiency with more sulfanilic acid can then be related to a faster degradation of larger quantities of organics with the consumption of greater amounts of generated hydroxyl radicals and the consequent deceleration of their parasitic reactions like reactions 9−12.

Comparison of results of parts a and b of Figure 3 corroborates that PEF has more oxidation power than EF for all sulfanilic acid concentrations. The PEF process allows achieving an almost total mineralization with a higher TOC removal of 97−98% after electrolysis times of 300, 360, and 540 min for 1.39, 6.95, and 13.9 mM, respectively. Again, the increase in substrate content causes a strong rise of its

dx.doi.org/10.1021/jp300442y | J. Phys. Chem. A 2012, 116, 3404−3412

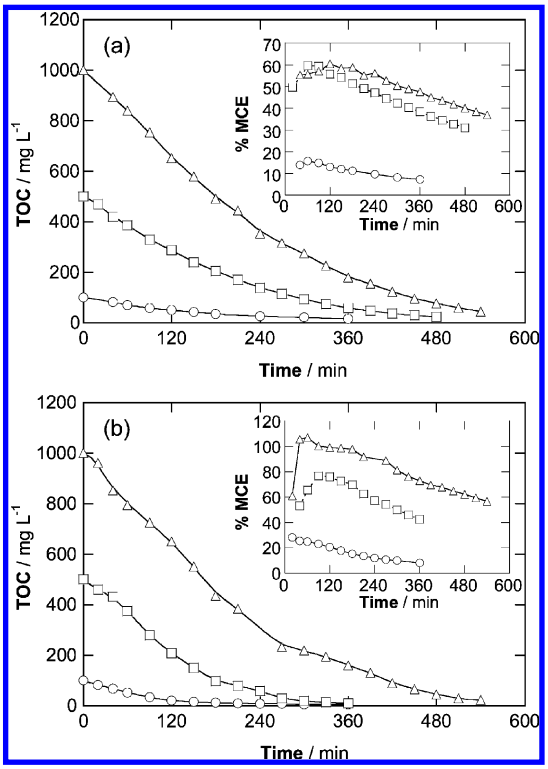

Figure 3. Effect of sulfanilic acid concentration on TOC decay for the (a) EF and (b) PEF degradations of 100 mL of solutions with 0.05 M Na_2SO_4 and 0.4 mM Fe^{2+} of pH 3.0 treated at 66.6 mA cm^{-2} and 35 °C. Substrate content: (○) 1.39 mM, (□) 6.95 mM, and (Δ) 13.9 mM. The mineralization current efficiency calculated from eq 7 is shown in the corresponding inset panels.

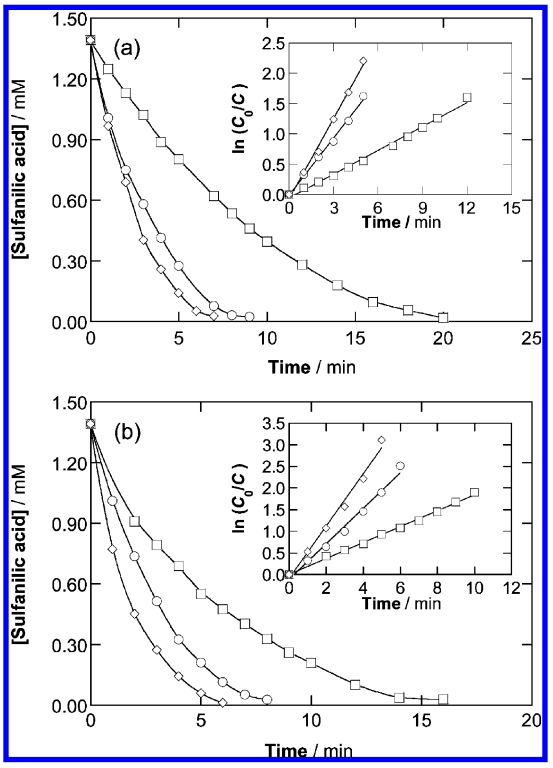

Figure 4. Influence of current density on the decay of sulfanilic acid concentration with electrolysis time during the treatment of a 1.39 mM solution by the (a) EF and (b) PEF treatments under the same conditions as given in Figure 2. Applied current density: (□) 33.3 mA cm^{-2}, (○) 66.6 mA cm^{-2}, and (◇) 100 mA cm^{-2}. The inset panels present the corresponding kinetic analysis considering a pseudo-first-order reaction for sulfanilic acid.

efficiency. The inset panel of Figure 3b illustrates a maximum MCE of 107% for the higher content of 13.9 mM treated by PEF, a value much higher than 60% found for EF (see the inset panel of Figure 3a). The higher efficiency for PEF is due to the quicker removal of organics by the additional production of •OH induced from reaction 5 and the fast photolysis of Fe(III)−carboxylate complexes, primordially at the first stages of the process. Note that the latter photochemical process is not considered in eq 7 to calculate MCE, and for this reason, it can reach a value as high as 107%.

The above findings allow establishing that PEF process is more preferable than EF for the degradation of sulfanilic acid in waters. The PEF process is more powerful, being able to yield almost total mineralization with higher TOC removal in less time under comparable conditions due to the synergistic action of UVA light.

3.3. Kinetics for Sulfanilic Acid Decay. The kinetics for the reaction between sulfanilic acid and electrogenerated hydroxyl radicals [•OH and BDD(•OH)] was followed by ion-exclusion HPLC, where it exhibited a well-defined peak at retention time (t_R) of 14.7 min. Blank experiments with and without 20 mM H_2O_2 under UVA illumination did not show any significant decay of sulfanilic acid, indicating that it is neither attacked by generated H_2O_2 nor directly photolyzed by UVA light in EF and PEF.

Figure 4 evidences the fast and complete destruction of 1.39 mM sulfanilic acid in both EAOPs, operating at optimum 0.4 mM Fe^{2+} and pH 3.0 for different current densities. Figure 4a shows that for EF, it disappears in 20, 9, and 7 min for 33.3, 66.6, and 100 mA cm^{-2}, respectively, whereas Figure 4b depicts a slightly quicker removal in 16, 8, and 6 min for the same current densities using PEF. The faster decay at higher current density can be accounted for by the gradual production of greater amounts of •OH in the bulk from Fenton's reaction 2 due to the larger H_2O_2 generation from reaction 1 and BDD(•OH) at the anode surface from reaction 4, in agreement with the higher TOC abatement shown under these conditions in Figure 2. The slight increase in rate of sulfanilic acid decay in the PEF process can then be ascribed to the additional generation of •OH induced from the photolytic reaction 5. The concentration decays for the above assays were well fitted to a pseudo-first-order kinetic equation, as shown in the inset panels of Figure 4a,b. From this kinetic analysis, pseudo-first-order rate constants (k_1) of 2.2×10^{-3} s^{-1} ($R^2 = 0.993$) for 33.3 mA cm^{-2}, 5.3×10^{-3} s^{-1} ($R^2 = 0.995$) for 66.6 mA cm^{-2}, and 7.4×10^{-3} s^{-1} ($R^2 = 0.994$) for 100 mA cm^{-2} using EF and 3.1×10^{-3} s^{-1} ($R^2 = 0.996$) for 33.3 mA cm^{-2}, 6.8×10^{-3} s^{-1} ($R^2 = 0.989$) for 66.6 mA cm^{-2}, and 1.0×10^{-2} s^{-1} ($R^2 = 0.989$) for 100 mA cm^{-2} using PEF were obtained. This behavior evidences a constant production of both reactive species •OH and BDD(•OH) at each current density in the EF and PEF processes, at least at the beginning of the electrolyses.

Figure 5 illustrates that in both EAOPs at 66.6 mA cm^{-2} under optimum conditions a longer time is needed for the total disappearance of sulfanilic acid when its concentration rises. For EF, it was completely removed in 9, 120, and 270 min for 1.39, 6.95, and 13.9 mM, respectively (see Figure 5a), whereas using PEF for these concentrations, its disappearance occurred at slightly smaller times of 8, 100, and 240 min (see Figure 5b),

dx.doi.org/10.1021/jp300442y | J. Phys. Chem. A 2012, 116, 3404−3412

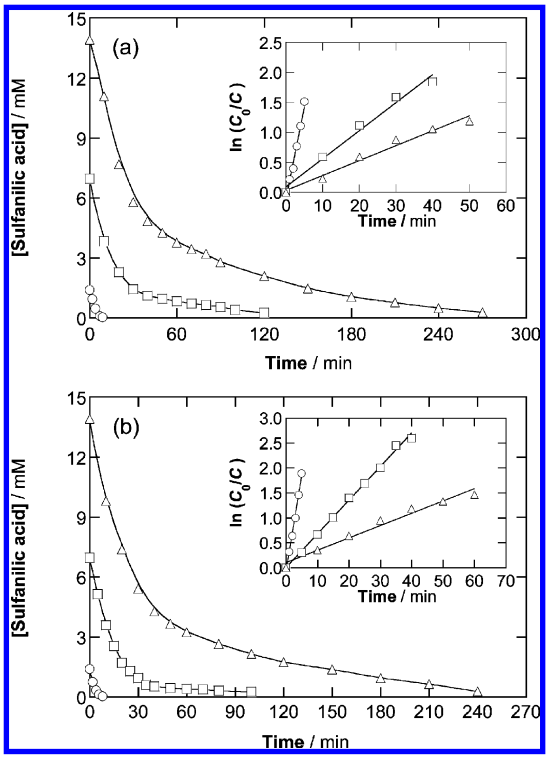

Figure 5. Effect of sulfanilic acid content on its decay kinetics for the (a) EF and (b) PEF degradations of (○) 1.39 mM, (□) 6.95 mM, and (Δ) 13.9 mM sulfanilic acid solution under the conditions of Figure 3 at 66.6 mA cm^{-2}. The kinetic analysis assuming that the substrate follows a pseudo-first-order reaction is given in the inset panels.

as a result of the extra production of $^{\bullet}OH$ induced by reaction 5 under UV irradiation. This is the expected trend in each EAOP because a longer time is expected to be required for the destruction of greater amounts of sulfanilic acid under similar generation of hydroxyl radicals. From the good linear correlations obtained assuming a pseudo-first-order reaction for this sulfonated amine, as shown in the inset panels of Figure 5a,b, decreasing k_1 values of 5.3×10^{-3} s^{-1} (R^2 = 0.995) for 1.39 mM, 7.8×10^{-4} s^{-1} (R^2 = 0.990) for 6.95 mM, and 4.1×10^{-4} s^{-1} (R^2 = 0.983) for 13.9 mM using EF as well as of 6.8×10^{-3} s^{-1} (R^2 = 0.989) for 1.39 mM, 1.1×10^{-3} s^{-1} (R^2 = 0.996) for 6.95 mM, and 4.3×10^{-4} s^{-1} (R^2 = 0.983) for 13.9 mM using PEF were found. The drop in k_1 when sulfanilic acid content increases suggests its gradual reaction with a smaller proportion of hydroxyl radicals because they attack more preferentially its intermediates, favoring the mineralization process and the efficiency enhancement, in agreement with the results reported in Figure 3.

3.4. Detection and Evolution of Intermediates.

Reversed-phase chromatograms recorded during the EF treatment of the 1.39 mM sulfanilic acid solution at different current densities displayed peaks related to hydroquinone at t_R = 3.5 min and *p*-benzoquinone at t_R = 5.3 min. Both aromatics were unequivocally identified by comparing their retention times and UV–vis spectra, measured on the photodiode array detector, with those of pure standards. It can then be assumed that the attack of hydroxyl radicals on the benzenic ring of sulfanilic acid causes its dihydroxylation on its C(1)- and C(4)-positions with direct loss of SO_4^{2-} and NH_4^+ ions yielding hydroquinone, which is subsequently oxidized to *p*-benzoquinone according to the following general reaction scheme:

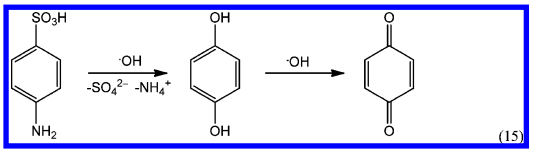

Figure 6a,b shows the evolution of hydroquinone and *p*-benzoquinone, respectively, for 33.3, 66.6, and 100 mA cm^{-2}.

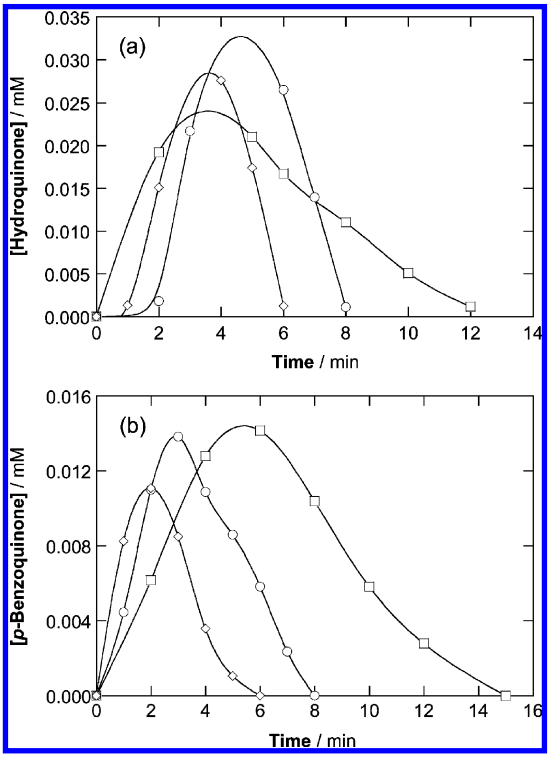

Figure 6. Evolution of (a) hydroquinone and (b) *p*-benzoquinone detected during the EF treatment of 100 mL of a 1.39 mM sulfanilic acid solution in 0.05 M Na_2SO_4 with 0.4 mM Fe^{2+} at pH 3.0 and 35 °C. Applied current density: (□) 33.3 mA cm^{-2}, (○) 66.6 mA cm^{-2}, and (◇) 100 mA cm^{-2}.

As can be seen, the former was accumulated to a larger extent than the latter at each current density, both compounds being destroyed more rapidly with increasing current density and disappearing at similar time to that of sulfanilic acid (see Figure 4a). However, the low maximum concentration reached for both compounds, 0.027 mM for hydroquinone and 0.014 mM for *p*-benzoquinone, indicates that their production was a minority, with a major proportion of other unidentified aromatics being formed from the attack of hydroxyl radicals on the initial substrate. Surprisingly, hydroquinone and *p*-benzoquinone were not detected during the comparative PEF degradations. This suggests that some intermediates originating hydroquinone are rapidly photolyzed with UVA light giving rise to other oxidation products.

It is well-known that the degradation of aromatics by EAOPs generates short-linear carboxylic acids.[7,23−25,35,36] The formation of these byproduct from sulfanilic acid was confirmed for the EF and PEF treatments of a 1.39 mM solution of this compound under optimized conditions at 66.6 mA cm^{-2}. Ion-exclusion chromatograms of such electrolyzed solutions displayed defined peaks corresponding to oxalic (t_R = 6.9 min), maleic (t_R = 8.2 min), oxamic (t_R = 9.4 min), formic (t_R = 13.7 min), and acetic (t_R = 15.6 min) acids. Maleic and acetic

dx.doi.org/10.1021/jp300442y | J. Phys. Chem. A 2012, 116, 3404−3412

acids are expected to be formed from the cleavage of the benzenic ring of intermediates, further being transformed into oxalic and formic acids.[23−26] Oxamic acid could then be formed from the breaking of aromatic moieties containing a $-NH_2$ group. Oxalic, oxamic, and formic acids are ultimate carboxylic acids that are directly oxidized to CO_2.[7,8]

Acetic acid was detected up to about 90 min of both EF and PEF processes with contents <0.011 mM, as expected if Fe(III)−acetate complexes are mainly destroyed by BDD(•OH).[7] In contrast, maleic and formic acids were only found during EF, reaching a maxima of 0.005 and 0.036 mM, respectively, and being completely removed in 90−120 min. That means that Fe(III)−maleate and Fe(III)−formate complexes are rapidly removed in PEF under the action of UVA irradiation. A different behavior can be observed in Figure 7a for oxalic acid, which persisted to the end of both EAOPs. This acid was accumulated until 0.21 mM at 90 min of EF, whereupon it decayed to 0.07 mM at 360 min due to the slow reaction of Fe(III)−oxalate complexes with BDD(•OH).[7] In PEF, however, these species were rapidly photodecomposed by UVA light following reaction 6 and oxalic acid was completely destroyed in 360 min, i.e., when the treated solution was almost totally mineralized (see Figure 2b). Figure 7b reveals that in both EF and PEF treatments, oxamic acid attained a final content of ca. 0.01 mM after reaching a maximum value of 0.05 mM at 120 min, indicating that Fe(III)−oxamate species are destroyed by hydroxyl radicals without significant photolysis by UVA irradiation. A simple mass balance at 240 min of EF and PEF revealed that the content of both oxalic and oxamic acids was equivalent to 3.5 and 1.4 mg L^{-1} TOC, respectively, values much lower than 25.8 and 8.0 mg L^{-1} TOC found for the corresponding treated solutions (see Figure 2a,b). This allows concluding that greater amounts of other undetected recalcitrant organics are present in the solutions treated by both EAOPs at long electrolysis time.

3.5. Time-Course of Released Inorganic Nitrogen Ions.

The mineralization of *N*-compounds by EAOPs occurs alongside the release of inorganic ions like NH_4^+ and NO_3^-.[7,14,21,23−25] The production of both ions during the degradation of 1.39 mM sulfanilic acid with 0.4 mM Fe^{2+} at pH 3.0 by EF and PEF at 66.6 mA cm^{-2} was corroborated by ionic chromatography, without detecting the presence of other inorganic nitrogen ions such as NO_2^-. From the comparison of parts c and d of Figure 7, one can infer that NH_4^+ ion was always preferentially generated in relation to NO_3^- ion, even in larger proportion in the PEF process, as proposed in reaction 8. The major part of both ions was released during the first 120 min of both treatments, and at 360 min of electrolysis, the solution treated by EF contained 1.21 mM of NH_4^+ (87% of initial N) and 0.045 mM of NO_3^- (3% of initial N), whereas that degraded by PEF contained 1.32 mM of NH_4^+ (95% of initial N) and 0.024 mM of NO_3^- (2% of initial N). The loss of 97% of initial N as NH_4^+ and NO_3^- ions in PEF when the solution is almost completely mineralized with 95% TOC decay (see Figure 2b) evidences that all initial N is mineralized without significant release of volatile *N*-compounds. Consequently, the fact that 90% of initial N is only converted into NH_4^+ and NO_3^- ions in EF when 85% TOC is removed from the solution (see Figure 2a) suggests that about 10% of the initial N content still remains in the solution as recalcitrant *N*-derivatives.

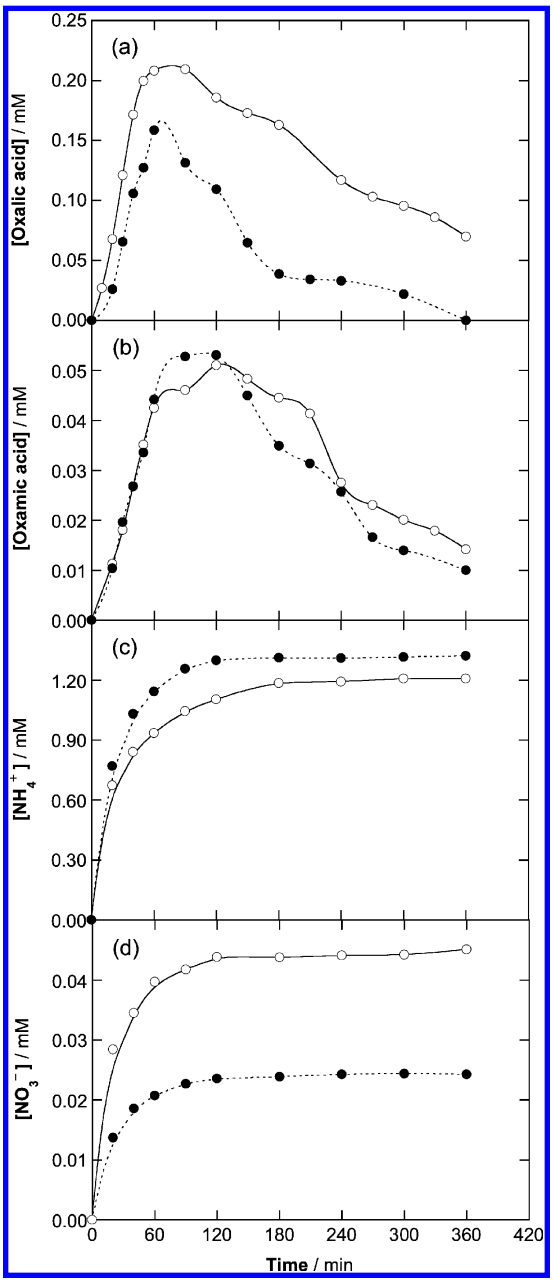

Figure 7. Time-course of (a) oxalic acid, (b) oxamic acid, (c) ammonium ion, and (d) nitrate ion during the degradation of 100 mL of a 1.39 mM sulfanilic acid solution in 0.05 M Na_2SO_4 with 0.4 mM Fe^{2+} at pH 3.0, 66.6 mA cm^{-2}, and 35 °C by (○) EF and (●) PEF.

4. CONCLUSIONS

It has been demonstrated that the PEF process is more powerful than the EF one to mineralize sulfanilic acid. Solutions with 1.39 mM of this compound were partially decontaminated by means of the EF treatment up to 100 mA cm^{-2}. Optimum conditions were achieved by operating with 0.4 mM Fe^{2+} and at pH 3.0. The increase in current density and substrate content led to an almost total mineralization with about 95% TOC removal. The use of PEF enhanced the degradation process and an almost complete mineralization until 97−98% TOC decay was obtained in less electrolysis time under comparable conditions. The mineralization current efficiency decreased with increasing current density and less initial substrate content, achieving a maximum value as high as 107% for a 13.9 mM

dx.doi.org/10.1021/jp300442y | J. Phys. Chem. A 2012, 116, 3404−3412

solution degraded by PEF at 66.6 mA cm^{-2}. The kinetics for sulfanilic acid decay always followed a pseudo-first-order reaction. Its apparent constant rate was slightly higher for PEF due to the additional production of $^{\bullet}OH$ from Fenton's reaction 2 induced by reaction 5. Low concentrations of the aromatic intermediates hydroquinone and *p*-benzoquinone were detected only in EF by reversed-phase HPLC, which were totally removed while sulfanilic acid disappeared. Acetic, maleic, formic, oxalic, and oxamic acids were identified as generated carboxylic acids by ion-exclusion HPLC. The two latter acids persisted to the end of both treatments, although Fe(III)−oxalate complexes were completely removed in PEF owing to their rapid photodecomposition under UVA irradiation. The higher mineralization power of PEF compared with EF can then be explained by the photolysis of Fe(III)−carboxylate complexes by UVA light. The initial N was preferentially converted into NH_4^+ ion and in much smaller proportion into NO_3^- ion.

AUTHOR INFORMATION

Corresponding Author

*Tel: +34 934021223. Fax: +34 934021231. E-mail: brillas@ub.edu.

Notes

The authors declare no competing financial interest.

ACKNOWLEDGMENTS

The authors acknowledge the grant given to A.E.G. and the financial support from MICINN (Ministerio de Ciencia e Innovación, Spain) through project CTQ2010-16164/BQU, cofinanced with FEDER funds.

REFERENCES

(1) Tarr, M. (Ed.) *Chemical Degradation Methods for Wastes and Pollutants. Environmental and Industrial Applications*; Marcel Dekker: New York, 2003.

(2) Brillas, E.; Calpe, J. C.; Cabot, P. L. *Appl. Catal. B-Environ.* **2003**, *46*, 381−391.

(3) Pera-Titus, M.; García-Molina, V.; Baños, M. A.; Giménez, J.; Esplugas, S. *Appl. Catal. B-Environ.* **2004**, *47*, 219−256.

(4) Klavarioti, M.; Mantzavinos, D.; Kassinos, D. *Environ. Int.* **2009**, *35*, 402−417.

(5) Martínez-Huitle, C. A.; Ferro, S. *Chem. Soc. Rev.* **2006**, *35*, 1324−1340.

(6) Martínez-Huitle, C. A.; Brillas, E. *Angew. Chem., Int. Ed.* **2008**, *47*, 1998−2005.

(7) Brillas, E.; Sirés, I.; Oturan, M. A. *Chem. Rev.* **2009**, *109*, 6570−6631.

(8) Panizza, M.; Cerisola, G. *Chem. Rev.* **2009**, *109*, 6541−6569.

(9) Diagne, M.; Oturan, N.; Oturan, M. A. *Chemosphere* **2007**, *66*, 841−848.

(10) Khataee, A. R.; Zarei, M.; Asl, S. K. *J. Electroanal. Chem.* **2010**, *648*, 143−150.

(11) Zarei, M.; Khataee, A. R.; Ordikhani-Seyedlar, R.; Fathinia, M. *Electrochim. Acta* **2010**, *55*, 7259−7265.

(12) Khataee, A. R.; Safarpour, M.; Zarei, M.; Aber, S. *J. Electroanal. Chem.* **2011**, *659*, 63−68.

(13) Oturan, N.; Oturan, M. A. *Agron. Sustainable Dev.* **2005**, *25*, 267−270.

(14) Hammami, S.; Bellakhal, N.; Oturan, N.; Oturan, M. A.; Dachraoui, M. *Chemosphere* **2008**, *73*, 678−684.

(15) Özcan, A.; Şahin, Y.; Koparal, A. S.; Oturan, M. A. *Appl. Catal. B-Environ.* **2009**, *89*, 620−626.

(16) Sirés, I.; Oturan, N.; Oturan, M. A. *Water Res.* **2010**, *44*, 3109−3120.

(17) Oturan, M. A.; Oturan, N.; Edelahi, M. C.; Podvorica, F. I.; El Kacemi, K. *Chem. Eng. J.* **2011**, *171*, 127−135.

(18) Wang, A.; Qu, J.; Liu, H.; Ru, J. *Appl. Catal. B-Environ.* **2008**, *84*, 393−399.

(19) Cruz-González, K.; Torres-López, O.; García-León, A.; Guzmán-Mar, J. L.; Reyes, L. H.; Hernández-Ramírez, A.; Peralta-Hernández, J. M. *Chem. Eng. J.* **2010**, *160*, 199−206.

(20) Boye, B.; Dieng, M. M.; Brillas, E. *Electrochim. Acta* **2003**, *48*, 781−790.

(21) Ammar, S.; Abdelhedi, R.; Flox, C.; Arias, C.; Brillas, E. *Environ. Chem. Lett.* **2006**, *4*, 229−233.

(22) Panizza, M.; Cerisola, G. *Water Res.* **2009**, *43*, 339−344.

(23) Isarain−Chávez, E.; Arias, C.; Cabot, P. L.; Centellas, F.; Rodríguez, R. M.; Garrido, J. A.; Brillas, E. *Appl. Catal. B-Environ.* **2010**, *96*, 361−369.

(24) Borràs, N.; Oliver, R.; Arias, C.; Brillas, E. *J. Phys. Chem. A* **2010**, *114*, 6613−6621.

(25) Isarain-Chávez, E.; Garrido, J. A.; Rodríguez, R. M.; Centellas, F.; Arias, C.; Cabot, P. L.; Brillas, E. *J. Phys. Chem. A* **2011**, *115*, 1234−1242.

(26) Marselli, B.; García-Gomez, J.; Michaud, P. A.; Rodrigo, M. A.; Comninellis, Ch. *J. Electrochem. Soc.* **2003**, *150*, D79−D83.

(27) Cañizares, P.; García-Gómez, J.; Lobato, J.; Rodrigo, M. A.. *Ind. Eng. Chem. Res.* **2003**, *42*, 956−962.

(28) Polcaro, A. M.; Vacca, A.; Mascia, M.; Palmas, S. *Electrochim. Acta* **2005**, *50*, 1841−1847.

(29) Flox, C.; Cabot, P. L.; Centellas, F.; Garrido, J. A.; Rodríguez, R. M.; Arias, C.; Brillas, E. *Chemosphere* **2006**, *64*, 892−902.

(30) Panizza, M.; Barbucci, A.; Ricotti, R.; Cerisola, G. *Sep. Purif. Technol.* **2007**, *54*, 382−387.

(31) Sirés, I.; Brillas, E.; Cerisola, G.; Panizza, M. *J. Electroanal. Chem.* **2008**, *613*, 151−159.

(32) Cañizares, P.; Paz, R.; Sáez, C.; Rodrigo, M. A. *Electrochim. Acta* **2008**, *53*, 2144−2153.

(33) Flox, C.; Arias, C.; Brillas, E.; Savall, A.; Groenen-Serrano, K. *Chemosphere* **2009**, *74*, 1340−1347.

(34) Hamza, M.; Abdelhedi, R.; Brillas, E.; Sirés, I. *J. Electroanal. Chem.* **2009**, *627*, 41−50.

(35) Skoumal, M.; Rodríguez, R. M.; Cabot, P. L.; Centellas, F.; Garrido, J. A.; Arias, C.; Brillas, E. *Electrochim. Acta* **2009**, *54*, 2077−2085.

(36) Ruiz, E. J.; Arias, C.; Brillas, E.; Hernández-Ramírez, A.; Peralta-Hernández, J. M. *Chemosphere* **2011**, *82*, 495−501.

(37) Zuo, Y.; Hoigné, J. *Environ. Sci. Technol.* **1992**, *26*, 1014−1022.

(38) Coughlin, M. F.; Kinkle, B. K.; Bishop, P. L. *Water Res.* **2003**, *37*, 2757−2763.

(39) Yemashova, N.; Telegina, A.; Kotova, I.; Netrusov, A.; Kalyuzhnyi, S. *Appl. Biochem. Biotechnol.* **2004**, *119*, 31−40.

(40) Tan, N. C. G.; van Leeuwen, A.; van Voorthuizen, E. M.; Slenders, P.; Prenafeta-Boldu, F. X.; Temmink, H.; Lettinga, G.; Field, J. A. *Biodegradation* **2005**, *16*, 527−537.

(41) Perei, K.; Rakhely, G.; Kiss, I.; Polyak, B.; Kovacs, K. L. *Appl. Microbiol. Biotechnol.* **2001**, *55*, 101−107.

(42) Singh, P.; Mishra, L. C.; Pandey, A.; Iyengar, L. *Biores. Technol.* **2006**, *97*, 1655−1659.

(43) Wang, Y. Q.; Zhang, J. S.; Zhou, J. T.; Zhang, Z. P. *J. Hazard. Mater.* **2009**, *169*, 1163−1167.

(44) Ming, G. H.; Shafinaz, S.; Zaharah, I.; Adibah, Y. *Chemosphere* **2011**, *82*, 507−513.

(45) Gul, S.; Serindag, O.; Boztepe, H. *Turk. J. Chem.* **1999**, *23*, 21−26.

(46) Santos, V.; Diogo, J.; Pacheco, M. J. A.; Ciríaco, L.; Morão, A.; Lopes, A. *Chemosphere* **2010**, *79*, 637−645.

(47) Hu, L.; Flanders, P. M.; Miller, P. L.; Strathmann, T. J. *Water Res.* **2007**, *41*, 2621−2626.

(48) Marciocha, D.; Kalka, J.; Turek-Szytow, J.; Wiszniowski, J.; Surmacz-Gorska, J. *Water Sci. Technol.* **2009**, *60*, 2555−2562.

(49) Carvalho, C.; Fernandes, A.; Lopes, A.; Pinheiro, H.; Gonçalves, I. *Chemosphere* **2007**, *67*, 1316−1324.

(50) Brillas, E.; Baños, M. A.; Camps, S.; Arias, C.; Cabot, P. L.; Garrido, J. A.; Rodríguez, R. M. *New J. Chem.* **2004**, *28*, 314−322.
(51) Skoumal, M.; Arias, C.; Cabot, P. L.; Centellas, F.; Garrido, J. A.; Rodríguez, R. M.; Brillas, E. *Chemosphere* **2008**, *71*, 1718−1729.